



Discovery and optimization of piperidyl benzamide derivatives as a novel class of 11 β -HSD1 inhibitors

Yosup Rew^{*}, Dustin L. McMinn, Zhulun Wang, Xiao He, Randall W. Hungate, Juan C. Jaen[†], Athena Sudom, Daqing Sun, Hua Tu, Stefania Ursu, Elisia Villemure, Nigel P. C. Walker, Xuelei Yan, Qiuping Ye, Jay P. Powers[†]

Amgen Inc., 1120 Veterans Boulevard, South San Francisco, CA 94080, USA

ARTICLE INFO

Article history:

Received 16 December 2008

Revised 15 January 2009

Accepted 16 January 2009

Available online 23 January 2009

Keywords:

11 β -HSD1

Type II diabetes

Insulin sensitivity

Cyclohexyl benzamide

Piperidyl benzamide

PXR

Microsomal stability

Hepatocyte stability

ABSTRACT

Discovery and optimization of a piperidyl benzamide series of 11 β -HSD1 inhibitors is described. This series was derived from a cyclohexyl benzamide lead structures to address PXR selectivity, high non-specific protein binding, poor solubility, limited in vivo exposure, and in vitro cytotoxicity issues observed with the cyclohexyl benzamide structures. These efforts led to the discovery of piperidyl benzamide **15** which features improved properties over the cyclohexyl benzamide derivatives.

© 2009 Elsevier Ltd. All rights reserved.

One of the key regulatory roles of glucocorticoids is glucose homeostasis. In this regard, glucocorticoids regulate gluconeogenesis in the liver and inhibit peripheral glucose uptake in muscle and adipose tissue. 11 β -Hydroxysteroid dehydrogenase type 1 (11 β -HSD1), an NADPH-dependent reductase, is a key enzyme that converts the inactive glucocorticoid cortisone to the active glucocorticoid hormone cortisol in liver, adipose, and brain tissues. Excessive concentrations of glucocorticoids in the liver and adipose tissue can lead to glucose intolerance and insulin resistance. Therefore, selective inhibition of the 11 β -HSD1 enzyme has been considered as a promising strategy to improve insulin sensitivity and treat type II diabetes.^{1,2}

Previously we reported on a series of cyclohexyl benzamide derivatives, exemplified by compound **1**, as potent 11 β -HSD1 inhibitors (Fig. 1).³ Compound **1** exhibited excellent in vitro inhibition of human 11 β -HSD1 enzyme and favorable pharmacokinetic profiles in the rat, cynomolgus monkey, and dog. Furthermore, compound **1** showed a dose-dependent decrease in adipose 11 β -HSD1 activity in a monkey ex vivo pharmacodynamic model.³

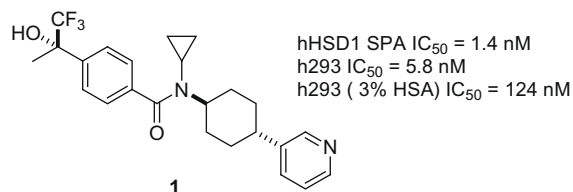


Figure 1. Representative cyclohexyl benzamide 11 β -HSD1 inhibitor.^{3,8}

However, **1** exhibited low micromolar range in vitro cytotoxicity in HeLa cells (IC₅₀ = 2.5 μ M).⁴

The X-ray co-crystal structure of **1** with the 11 β -HSD1 enzyme showed that the pyridyl ring points toward the solvent exposed region of the protein dimer interface and does not make any discernable specific interaction with the active site of the protein.³ Combined with our initial SAR,³ this gave some indication that the core cyclohexyl benzamide motif was the essential binding component of these molecules. We hypothesized that, by replacing the pyridyl group with other functional groups, we could modulate physicochemical properties without disrupting critical interactions with the enzyme. Moreover, in addition to enhancing the structural diversity of compounds at the 4-position of the cyclohexane ring,

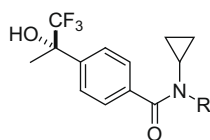
^{*} Corresponding author. Tel.: +1 650 244 2682.

E-mail address: yrew@amgen.com (Y. Rew).

[†] Currently at ChemoCentryx, Inc., Mountain View, CA 94043, USA.

Table 1

SAR of cyclohexyl and piperidyl benzamides with polar alkyl substituents



Compound ^a	R	hHSD1 SPA ^b IC ₅₀ (nM)	h293 ^c (cell) IC ₅₀ (nM)	h293 (cell, 3% HSA ^d) IC ₅₀ (nM)	% Remaining z@ 30 min		PXR ^g activation % of control ^h @ 2 μM	HeLa cytotoxicity IC ₅₀ (μM)
					hLM ^e	rLM ^f		
2		5.5	16	60	>90	73	75	N/D ⁱ
3		7.6	52	202	70	5	74	N/D
4		0.7	1.4	11	>90	42	30	>10
5		2.8	10	130	64	<5	56	>10
6		0.88	1.4	30	>90	77	60	N/D
7		2.0	8	129	N/D	N/D	N/D	N/D
8		0.6	1.2	28	>90	>90	60	4
9		36	315	1190	N/D	N/D	1	N/D
	(trans/cis = 1/1)							
10		2.4	17	77	>90	>90	5	>10
11		11	109	417	>90	72	100	>10
12		3.8	6.1	97	>90	>90	4	>10
13		1.7	5.0	90	>90	>90	6.5	8
14		11	56	108	86	28	3	>10
15		14	167	148	>90	86	4	>10

^{b,c,d} All potency data are reported as the average of at least two determinations.^a All compounds gave satisfactory ¹H NMR, HPLC, and MS data in full agreement with their proposed structures, and purity (>95%) was determined by HPLC analysis.^b IC₅₀ values determined by scintillation proximity assay.^c h293 = HEK 293 cells stably transfected with full-length human 11β-HSD1.^d HSA = human serum albumin.^e hLM = human liver microsomes.^f rLM = rat liver microsomes.^g PXR = pregnane X receptor.^h Rifampin (@ 10 μM) used as a positive control.ⁱ N/D = not determined.

such modifications would potentially offer an opportunity to address the off-target cytotoxicity observed in HeLa cells without affecting the 11 β -HSD1 activity.

We felt that extending polar groups from the 4-position of the cyclohexyl ring would enhance the solubility of the compounds. We therefore initiated our efforts by the systematic introduction of polarity via carbon tethered nitrile and primary amide groups (compounds **2–13** in Table 1).

Compounds **2–13** were synthesized via the routes outlined in Scheme 1. Three cyclohexylamine intermediates (**18a–18c**) were prepared from the monoacetal (**16**). Reaction of diethyl cyanomethylphosphonate sodium salt with **16**, followed by hydrogenation afforded nitrile **17**.⁵ In a similar manner, **16** was transformed into ester **19**, which was followed by carbon-chain elongation of **19** to provide homologated nitrile **20**.⁶ α,α -Dimethyl-nitrile **21** was prepared via sequential methylation of **20**. The corresponding cyclopropyl analog **24** was synthesized by conversion

of ester **22** into bromide **23** followed by alkylation of **23** with the cyclopropanecarbonitrile anion.⁷ All these protected ketone intermediates (**17**, **20**, **21**, and **24**) were converted into amines **18a–18d** by removal of the ketal protecting group, followed by reductive amination with cyclopropylamine. Finally, the target 4-cyanoalkyl-cyclohexyl benzamides, **2–8** were synthesized via amide coupling reaction of these amines with chiral acid **25**³ followed by separation of each geometric isomer (*cis* and *trans*) using silica-gel column chromatography. Further hydrolysis of the cyano group to the primary amide provided carboxamide derivatives, **9–13**.

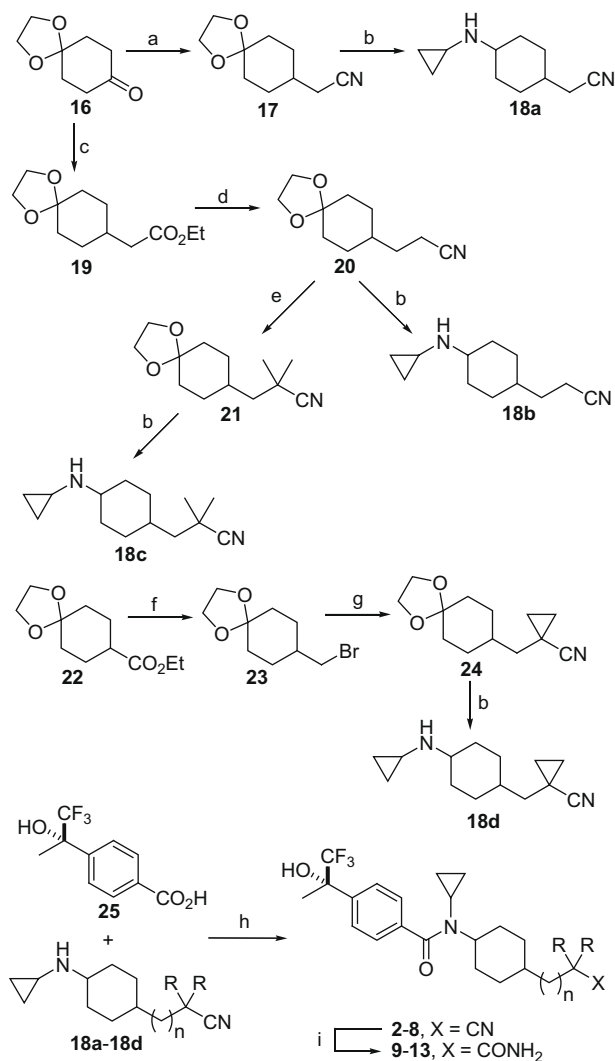
All synthesized compounds were evaluated for the inhibition of human and mouse 11 β -HSD1 enzymes, as well as in cell-based assays.⁸ Consistent with our previous publication,³ *trans* isomers (**2**, **4**, **6**, **10**) were typically more potent than *cis* isomers (**3**, **5**, **7**, **11**) in both biochemical and cellular assays. A 2-carbon spacer length between the polar functional group ($-\text{CN}$ or $-\text{CONH}_2$) and the cyclohexane ring resulted in a substantial increase in potency relative to the 1-carbon spacer (**2**, **3** vs **4**, **5**). The improvement in biochemical potency for **4** and **5** may reflect a greater tolerance of polar features distanced further towards solvent exposed regions of the protein. Within the 2-carbon linked nitrile and primary amide molecules, both biochemical potency and cellular potency were slightly decreased in primary amides (**10**, **11**, **12**, **13**) relative to the corresponding nitriles (**4**, **5**, **6**, **8**). Also, compounds in this series showed 5- to 20-fold shift in their IC_{50} values in the h293 cell-based assays upon addition of HSA.

As observed previously in mono-substituted cyclohexyl benzamides,³ *trans* isomers were found to be more metabolically stable than *cis* isomers in both human liver microsomes and rat liver microsomes (**2**, **4**, **10** vs **3**, **5**, **11**). Replacement of the nitrile group with a primary amide improved the rat in vitro metabolic stability significantly (**4**, **6** vs **10**, **12**), while installation of α,α -disubstituents such as *gem*-dimethyl or cyclopropyl group further enhanced in vitro metabolic stability in rat (**4** vs **6**, **8**).

Compounds were also evaluated for their potential to activate PXR, a liability that can potentially lead to upregulation of CYP3A4.⁹ In most cases, *trans* isomers exhibited reduced PXR activity in vitro (**4**, **10** vs **5**, **11**), while conversion of the nitrile group to the more polar primary amide group in *trans* isomers significantly reduced PXR activation potential (**2**, **4**, **6**, **8** vs **9**, **10**, **12**, **13**).

Of significance was the observation that most compounds evaluated had marked reduction in cytotoxicity ($\text{IC}_{50} \geq 10 \mu\text{M}$) relative to **1**. Moreover, compounds **10** and **12** showed optimal combination of limited cytotoxicity and PXR potential, good potency and microsomal stability and were therefore selected for rat pharmacokinetic (PK) studies.^{10a,10b} However, it was found that the in vitro rat liver microsomal stability of **10** and **12** (>90% remaining after 30 min for both **10** and **12**) was not predictive of the in vivo rat clearance. Compounds **10** and **12** were found to have high and moderate clearance in rat [CL (iv) = 3.0 and 1.3 L/h/kg, respectively] in addition to moderate oral bioavailability (%F = 22 and 32, respectively).

Metabolic studies utilizing compound **10** with human and rat hepatocytes revealed that hydrolysis of the primary amide to the corresponding carboxylic acid occurred, followed by glucuronidation to **27** (Fig. 2). This observation provided an explanation for the disconnect between the observed in vitro microsomal stability and the rat in vivo clearance. Introduction of α,α -dialkyl substituents improved in vitro stability in both human and rat hepatocytes (**10** vs **12**). Moreover, replacement of the *gem*-dimethyl group with a cyclopropyl group significantly enhanced the in vitro hepatocyte stability in human and rat (Table 2). This superior stability of the cyclopropyl compound **13** relative to the *gem*-dimethyl compound **12** can potentially be explained by a combination of steric and electronic effects.¹¹



Scheme 1. Reagents and conditions: (a) i— $(\text{EtO})_2\text{P}(\text{O})\text{CH}_2\text{CN}$, NaH, DMPU, THF, 95%; ii—10% Pd/C, H₂, AcOH/H₂O, 95%; (b) i—a 1:2 (v/v) mixture of 3 N aqueous HCl and THF, quantitatively; (ii) cyclopropylamine, NaBH(OAc)₃, AcOH, 1,2-DCE, 80–95%; (c) i— $(\text{EtO})_2\text{P}(\text{O})\text{CH}_2\text{CO}_2\text{Me}$, NaH, DMPU, THF, 85%; ii—10% Pd/C, H₂, EtOAc, 98%; (d) i—LiAlH₄, ether, 91%; ii—MeCl, TEA, DCM, quantitatively; iii—NaCN, DMSO, 71%; (e) i—LDA, MeI, THF, 76%; ii—LDA, MeI, THF, 70%; (f) i—NaBH₄, 10% MeOH-DME, 77%; ii—CBr₄, Ph₃P, benzene, 81%; (g) LDA, cyclopropanecarbonitrile, THF, –78 °C, 63%; (h) HBTU, HOBT, DIEA, DMF, 30–60% (*cis*/*trans* = 1/1–7.8/1); i—KOH, *t*-BuOH, 85 °C, 48–81%.

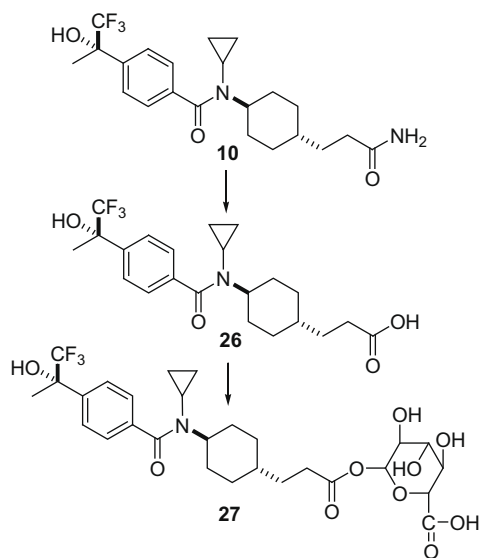


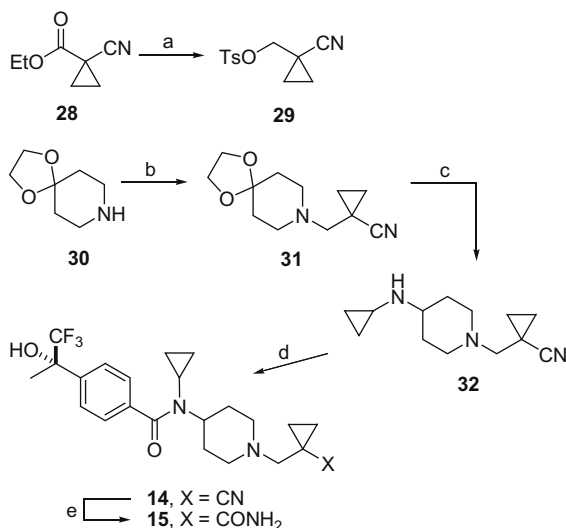
Figure 2. Metabolism of compound **10** in human and rat hepatocytes.

Table 2
In vitro hepatocyte stability of compounds **10**, **12**, and **13**

Compound	Hepatocyte stability % remaining @ 90 min	
	hHep ^a	rHep ^b
10	32	<5
12	84	10
13	>90	73

^a hHep = human hepatocytes.

^b rHep = rat hepatocytes.



Scheme 2. Reagents and conditions: (a) i) NaBH_4 , 10% MeOH–DME, 90%; ii) TsCl , pyridine, 0 °C, 75%; (b) **29**, DIEA, AcCN, 85 °C, 80%; (c) (i) 5% H_2O –TFA, 88%; ii–cyclopropylamine, $\text{NaBH}(\text{OAc})_3$, AcOH, 1,2-DCE, 100%; (d) **25**, EDCI, HOAt, NaHCO_3 , DMF, 74%; (e) KOH, t -BuOH, 85 °C, 45%.

Having identified a pendant feature that appeared well tolerated and stable in hepatocytes, an effort was made to further enhance solubility and stereosimplicity by optimization of the cyclopropylamide in the context of a more polar piperidine ring architecture.

Piperidyl benzamide derivatives, **14** and **15** were synthesized in a straightforward manner, through a sequence illustrated in

Scheme 2. Ethyl 1-cyanocyclopropanecarboxylate **28** was prepared according to the literature procedures¹² and was converted into tosylate **29** following ester reduction. *N*-Alkylation of piperidine **30** with **29** provided **31**. Ketal hydrolysis followed by reductive amination afforded amine intermediate **32**. Amide coupling of **32** with chiral acid **25** yielded *N*-cyanoalkylpiperidyl benzamide **14**, which was transformed into the primary amide derivative **15**.

The potency and biological data of compound **14** and **15** are summarized in Table 1. Both **14** and **15** were less potent than the corresponding cyclohexyl benzamides in both biochemical and cellular assays (**14**, **15** vs **8**, **13**). However, piperidyl benzamides showed a much lower cellular potency shift upon addition of HSA (1- to 2-fold shift) compared to cyclohexyl benzamides and their cellular potency in the presence of 3% HSA was comparable to that of **13**. Plasma protein binding data for compound **13** and **15** are also consistent with the cellular potency shift upon addition of HSA (Table 3).

Whereas **14** showed a compromised in vitro metabolic stability in rats, the cyclopropyl amide **15** had improved metabolic stability. Compound **15** was evaluated in rat pharmacokinetic studies. Compound **15** exhibited low plasma clearance [$\text{CL}(\text{iv}) = 0.89 \text{ L/h/kg}$] and excellent oral bioavailability (%F = 69).^{10c} As with the cyclohexyl benzamide derivative, the in vitro human and rat hepatocyte stability assay results were in agreement with the in vivo plasma clearance of compound **15** (>90% remaining after 90 min in hHep, 69% remaining after 90 min in rHep).

The structure of compound **15** bound to human 11 β -HSD1 was determined by X-ray crystallography (Fig. 3) to a resolution of 2.3 Å.¹³ The co-crystal structure showed that the inhibitor binds to the substrate site in a V-shape with its trifluoromethylcarbinol

Table 3
Plasma protein binding for compounds **13** and **15**

Compound	fu in human plasma ^a	fu in rat plasma ^a
13	0.12	0.048
15	0.48	0.20

^a Samples analyzed on API-4000 and ultracentrifugation protocol-4 h. fu = fraction unbound.

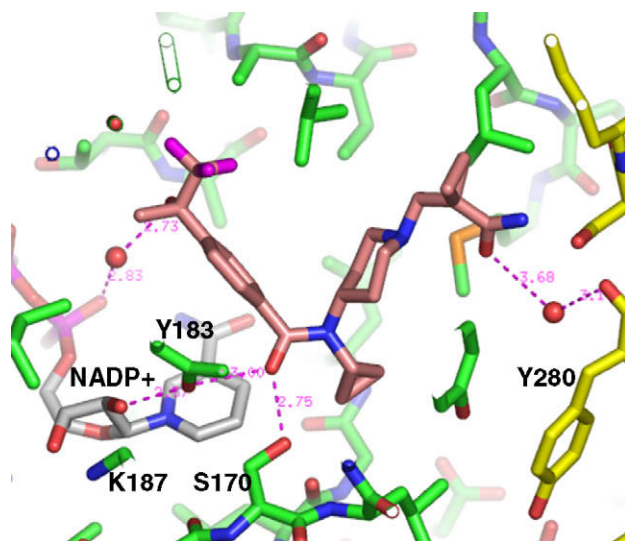


Figure 3. X-ray co-crystal structure of compound **15** in human 11 β -HSD1. The key hydrogen bonding interaction of **15** to the enzyme is shown with magenta dashed line. The color scheme is red for oxygen atoms, blue for nitrogen atoms, orange for sulfur atoms, magenta for fluorine atoms. Carbon atoms are in green for protein 1, yellow for protein 2, gray for NADP⁺, and beige for inhibitor. The water molecules are shown in red spheres.

group pointing towards the cofactor NADP⁺ side. The central amide carbonyl group makes a hydrogen bond interaction with the hydroxyl group of S170, one of the three residues defined as the catalytic triad for 11 β -HSD1 activity.¹⁴ The cyclopropanecarboxamide group locates in the dimer interface and forms a weak water-mediated hydrogen bond with C-terminal region of adjacent protein.

In summary, we have described our efforts towards the expansion of structural diversity and optimization of a structurally novel cyclohexyl benzamide series of 11 β -HSD1 inhibitors. Improvements in metabolic stability and reduction in cytotoxicity within the cyclohexyl benzamide series transferred well to the piperidyl subclass culminating in compound **15** which represents a potent and promising benzamide subclass. Compound **15** effectively addresses PXR activation, high non-specific protein binding, poor pharmacokinetic properties, and in vitro cytotoxicity issues previously observed with the cyclohexyl benzamide structures. This represents a promising step forward in our continued development of our benzamide class of 11 β -HSD1 inhibitors.

References and notes

- Recent reviews about 11 β -HSD1 target (a) Fotsch, C.; Wang, M. J. *Med. Chem.* **2008**, *51*, 4851; (b) Stulnig, T. M.; Waldhäusl, W. *Diabetologia* **2004**, *47*, 1; (c) Tomlinson, J. W.; Walker, E. A.; Bujalska, I. J.; Draper, N.; Lavery, G. G.; Cooper, M. S.; Hewison, M.; Stewart, P. M. *Endocr. Rev.* **2004**, *25*, 831; (d) Seckl, J. R.; Walker, E. A. *Trends Endocrinol. Metab.* **2004**, *15*, 418.
- Recent papers about 11 β -HSD1 target (a) Xiang, J.; Wan, Z.; Li, H.; Ipek, M.; Binnun, E.; Nunez, J.; Chen, L.; McKew, J. C.; Mansour, T. S.; Xu, X.; Suri, V.; Tam, M.; Xing, Y.; Li, X.; Hahm, S.; Tobin, J.; Saiah, E. J. *Med. Chem.* **2008**, *51*, 4068; (b) Johansson, L.; Fotsch, C.; Bartberger, M. D.; Castro, V. M.; Chen, M.; Emery, M.; Gustafsson, S.; Hale, C.; Hickman, D.; Homan, E.; Jordan, S. R.; Komorowski, R.; Li, A.; McRae, K.; Moniz, G.; Matsumoto, G.; Orihuela, C.; Palm, G.; Veniant, M.; Wang, M.; Williams, M.; Zhang, J. J. *Med. Chem.* **2008**, *51*, 2933; (c) Sun, D.; Zhulun, W.; Di, Y.; Jaen, J. C.; Labelle, M.; Ma, J.; Miao, S.; Sudom, A.; Tang, L.; Tomooka, C. S.; Tu, H.; Ursu, S.; Walker, N.; Yan, X.; Ye, Q.; Powers, J. P. *Bioorg. Med. Chem. Lett.* **2008**, *18*, 3513; (d) Wang, H.; Ruan, Z.; Li, J. J.; Simpkins, L. M.; Smirk, R. A.; Wu, S. C.; Hutchins, R. D.; Nirschl, D. S.; Kirk, K. V.; Cooper, C. B.; Sutton, J. C.; Ma, Z.; Golla, R.; Seethala, R.; Salyan, M. E. K.; Nayeem, A.; Krystek, S. R., Jr.; Sheriff, S.; Camac, D. M.; Morin, P. E.; Carpenter, B.; Robl, J. A.; Zahler, R.; Gordon, D. A.; Hamann, L. G. *Bioorg. Med. Chem. Lett.* **2008**, *18*, 3168; (e) Zhu, Y.; Olson, S. H.; Hermanowski-Vosatka, A.; Mundt, S.; Shah, K.; Springer, M.; Thieringer, R.; Wright, S.; Xiao, J.; Zokian, H.; Balkovec, J. M. *Bioorg. Med. Chem. Lett.* **2008**, *18*, 3405; (f) Rohde, J. J.; Plushchev, M. A.; Sorensen, B. K.; Wodka, D.; Shuai, Q.; Wang, J.; Fung, S.; Monzon, K. M.; Chiou, W. J.; Pan, L.; Deng, X.; Chovan, L. E.; Ramaiya, A.; Mullally, M.; Henry, R. F.; Stolarik, D. F.; Imade, H. M.; Marsh, K. C.; Beno, D. W. A.; Fey, T. A.; Droz, B. A.; Brune, M. E.; Camp, H. S.; Sham, H. L.; Frevert, E. U.; Jacobson, P. B.; Link, J. T. *J. Med. Chem.* **2007**, *50*, 149; (g) Yuan, C.; St. Jean, D. J., Jr.; Liu, Q.; Cai, L.; Li, A.; Han, N.; Moniz, G.; Askew, B.; Hungate, R. W.; Johansson, L.; Tedenborg, L.; Puring, D.; Williams, M.; Hale, C.; Chen, M.; Cupples, R.; Zhang, J.; Jordan, S.; Bartberger, M. D.; Sun, Y.; Emery, M.; Wang, M.; Fostch, C. *Bioorg. Med. Chem. Lett.* **2007**, *17*, 6056; (h) Sorensen, B.; Winn, M.; Rohde, J.; Shuai, Q.; Wang, J.; Fung, S.; Monzon, K.; Chiou, W.; Stolarik, D.; Imade, H.; Pan, L.; Deng, X.; Chovan, L.; Longenecker, K.; Judge, R.; Qin, W.; Brune, M.; Camp, H.; Frevert, E. U.; Jacobson, P.; Link, J. T. *Bioorg. Med. Chem. Lett.* **2007**, *17*, 527.
- Julian, L. D.; Wang, Z.; Bostick, T.; Caille, S.; Choi, R.; DeGraffenreid, M.; Di, Y.; He, X.; Hungate, R. W.; Jaen, J. C.; Liu, J.; Monshouwer, M.; McMinn, D.; Rew, Y.; Sudom, A.; Sun, D.; Tu, H.; Ursu, S.; Walker, N.; Yan, X.; Ye, Q.; Powers, J. P. *J. Med. Chem.* **2008**, *51*, 3953.
- Hela cytotoxicity assay: IC₅₀ for inhibition of cell growth of Hela cells at 72 hours was measured using Alamar blue assay.
- Yamamoto, T.; Eki, T.; Nagumo, S.; Suemune, H.; Saikai, K. *Tetrahedron* **1992**, *48*, 4517.
- Alonso, F.; Mico, I.; Najera, C.; Sansano, J. M.; Yus, M. *Tetrahedron* **1995**, *51*, 10259.
- Taber, D. F.; Bhamidipati, R. S.; Yet, L. J. *Org. Chem.* **1995**, *60*, 5537.
- 11 β -HSD1 enzyme activity was determined by measuring the conversion of [³H]-cortisone to [³H]-cortisol. Product [³H]-cortisol, captured by an anti-cortisol monoclonal antibody conjugated to scintillation proximity assay (SPA) beads, was quantified with a microscintillation plate reader. Biochemical enzyme assays were performed with Baculovirus-produced recombinant full-length human or mouse 11 β -HSD1 as the enzyme source and NADPH as cofactor. Cell-based enzyme assays (h293) utilized HEK293 cells stably expressing recombinant human full-length 11 β -HSD1 as the enzyme source without supplementation of NADPH. IC₅₀ values for enzyme inhibition were calculated with a dose response curve fitting algorithm with at least duplicate sets of samples. In the cellular assay, selected compounds were tested in the presence of human serum albumin (HSA) to measure the impact of protein binding.
- Pregnane X Receptor (PXR) assay: HepG2 cells transfected with a luciferase reporter construct driven by CYP3A4 gene and human PXR cDNA. Cells were exposed to test article and the luciferase activity determined by chemilum. Rifampin is used as control.
- a Compound **10**: dosed iv 0.51 mg/kg, po 2.0 mg/kg.; b Compound **12**: dosed iv 0.39 mg/kg, po 2.0 mg/kg.; c Compound **15**: dosed iv 0.50 mg/kg, po 2.0 mg/kg.
- Bender, D. M.; Peterson, J. A.; McCarthy, J. R.; Gunaydin, H.; Takano, Y.; Houk, K. N. *Org. Lett.* **2008**, *10*, 509.
- Husbands, S.; Fraser, W.; Suckling, C. J.; Wood, H. C. S. *Tetrahedron* **1995**, *51*, 865.
- The atomic coordinates have been deposited in the Protein Data Bank under an Accession Code 3FRJ.
- Hosfield, D. J.; Wu, Y.; Skene, R. J.; Hilgers, M.; Jennings, A.; Snell, G. P.; Aertgeerts, A. *J. Biol. Chem.* **2005**, *280*, 4639.